Directed Evolution and Unusual Protonation Mechanism of Pyridoxal Radical C–C Coupling Enzymes for the Enantiodivergent Photobiocatalytic Synthesis of Non-Canonical Amino Acids

Lei Cheng[1], Zhiyu Bo[1], Benjamin Krohn-Hansen[1], and Yang Yang[1,2]*

[1]Department of Chemistry and Biochemistry, University of California Santa Barbara, Santa Barbara, California 93106

[2]Biomolecular Science and Engineering Program, University of California Santa Barbara, Santa Barbara, California 93106

ABSTRACT: Visible light-driven pyridoxal radical biocatalysis has emerged as a new strategy for the stereoselective synthesis of valuable non-canonical amino acids in a protecting-group-free fashion. In our previously developed dehydroxylative C–C coupling using engineered PLP-dependent tryptophan synthases, an enzyme-controlled unusual α-stereochemistry reversal and pH-controlled enantiopreference were observed. Herein, through high-throughput photobiocatalysis, we evolved a set of stereochemically complementary PLP radical enzymes, allowing the synthesis of both L- and D-amino acids with enhanced enantiocontrol across a broad pH window. These newly engineered L- and D-amino acid synthases permitted the use of a broad range of organoboron substrates, including boronates, trifluoroborates and boronic acids, with excellent efficiency. Mechanistic studies unveiled unexpected PLP racemase activity with our earlier PLP enzyme variants. This promiscuous racemase activity was abolished in our evolved amino acid synthases, shedding light on the origin of enhanced enantiocontrol. Further mechanistic investigations suggest a switch of proton donor to account for the stereoinvertive formation of D-amino acids, highlighting an unusual stereoinversion mechanism which is rare in conventional two-electron PLP enzymology.

Introduction

Biocatalytic transformations are becoming increasingly integral to synthetic chemistry, providing an efficient and selective alternative to traditional chemical synthesis while offering a complementary retrosynthetic logic.[1-4] The past decade has witnessed the development of a variety of synthetically valuable biocatalytic processes which were not known in native enzymology.[5-12] Among these, photobiocatalysis illuminates a new paradigm for exerting stereocontrol in free radical-mediated transformations, a challenging task that continues to elude small-molecular catalysts.[13-15] By capitalizing on the innate redox properties of natural cofactors including NAD(P)H[10, 16-18] and flavin[10, 19-42], through cofactor-based excited-state electron transfer, natural ketoreductases (KREDs),[16, 17] imine reductases (IREDs),[18] ene reductases (EREDs), [20-40] fatty acid photodecarboxylases (FAPs)[41] and cyclohexanone monooxygenases (CHMOs)[42] were successfully repurposed to catalyze unnatural stereoselective radical reactions. Very recently, by leveraging the synergy between photoredox catalysts and biocatalysts, our group and other researchers repurposed enzymes lacking a photoredox cofactor,[43-54] including pyridoxal 5'-phosphate (PLP)[48-51] and thiamine pyrophosphate (TPP)[53, 54]-dependent enzymes, to achieve stereoselective intermolecular asymmetric radical reactions with radicals generated outside the enzyme's active site.

Since 2023, using dual photobiocatalysis, our group has been advancing pyridoxal radical biocatalysis as a new platform for the stereoselective synthesis of non-canonical amino acids (ncAAs), which are essential building blocks of peptide therapeutics,[55-57] here bioactive natural products [58] and functional unnatural proteins.[59-64] By repurposing biotechnologically useful two-electron PLP enzymes[65-67] to catalyze single-electron transformations, pyridoxal radical biocatalysis allows the assembly of ncAAs via radical-mediated C–C coupling with excellent stereoselectivity.[48] Traditional chemical synthesis of ncAAs typically requires multistep protecting group manipulations for the amino and carboxylate moieties to ensure selective and efficient transformations.[68] In contrast, pyridoxal radical biocatalysis affords a protecting-group-free and convergent strategy for the preparation of ncAAs using abundant and inexpensive natural amino acid substrates and easily available radical precursors such as organoboron reagents. To date, we have reported the repurposing of two distinct classes of PLP enzymes, including tryptophan synthases[48] (type II PLP enzyme)[69-75] and threonine aldolases[49, 50] (type I PLP enzyme),[76, 77] to catalyze radical C–C coupling at the α and the β positions of amino acid substrates, respectively.

In 2023, we reported the stereoselective β-dehydroxylative C–C coupling of serine and threonine using engineered tryptophan synthase β-subunit variants to prepare ncAAs with up to three contiguous stereocenters under photobiocatalytic conditions[48]. An abbreviated mechanistic proposal is depicted in Scheme 1. Starting from the internal aldimine form **I** of tryptophan synthases β-subunit,[72, 73] transimination with the serine substrate (**2**) affords an external aldimine **II**. Lysine residue-mediated α-deprotonation of **II** furnishes a quinonoid intermediate **III**, which subsequently expels the β-hydroxy group to afford the key reactive, yet persistent, aminoacrylate **IV** stabilized by the protein scaffold. At this stage, externally formed transient carbon-centered radical **V** derived from the organoboron substrate **1** through single-electron oxidation mediated by the photoredox catalyst (rhodamine B, RhB) enters the enzyme active site, adding to the β position of aminoacylate **IV** in a stereocontrolled fashion. This leads to an azaallyl radical **VI**, which is subsequently converted to a new external aldimine **VII** upon single electron reduction and

enantioselective proton transfer. This external aldimine then releases the ncAA product **3** and regenerate the internal aldimine **I** upon transimination with the enzyme's conserved lysine residue, thereby completing the catalytic cycle.

Scheme 1. PLP-Dependent Tryptophan Synthase-Catalyzed Enantiodivergent Dehydroxylative Radical C–C Coupling

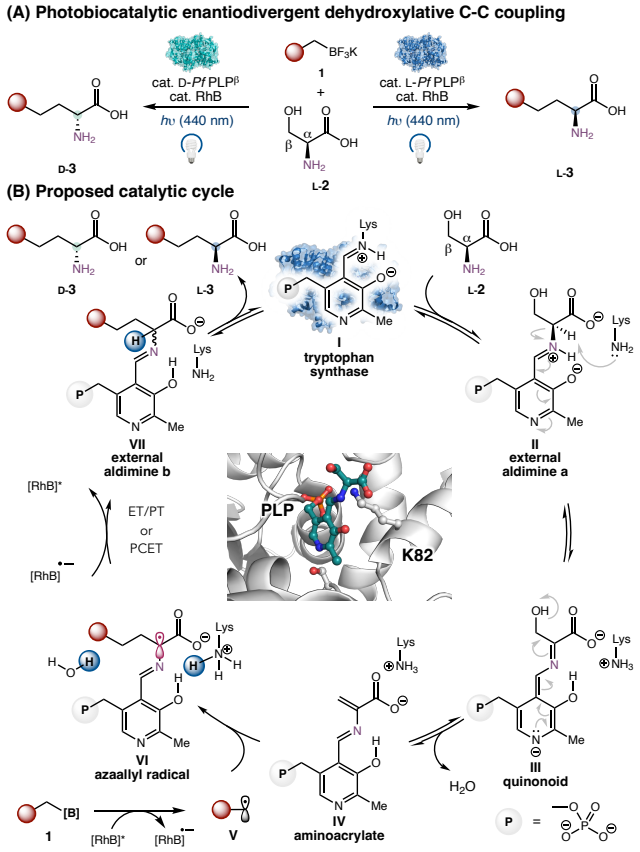

[a] *Pf*PLP$^{\beta}$ active-site structure was made using PDB # 5VMV. RhB = rhodamine B.

Despite the potential synthetic value of this dual photobiocatalytic system, many questions remain to be addressed. First, despite the tremendous success of directed evolution to optimize non-native enzyme functions,[5] there are relatively few examples on directed evolution of photobiocatalytic functions, particularly those requiring the use of both an enzyme and a small-molecule photoredox catalyst, via high-throughput experimentation (HTE).[46, 49, 54] In addition, in radical pyridoxal biocatalysis, through the use of a single mutant of the L-amino acid-producing variant L-*Pf*PLP$^{\beta}$, namely L-*Pf*PLP$^{\beta}$ E104G (D-*Pf*PLP$^{\beta}$), the unusual inversion of α-stereochemistry of amino acid products was achieved, giving rise to valuable *D-amino acids from L-serine* in a highly enantioenriched fashion. To date, this stereoinvertive β-pyridoxal radical biocatalysis continues to represent the only means to prepare D-amino acids from natural L- amino acid building blocks via a C–C bond formation process. [78,79] This stereochemical reversal is unusual, as in conventional PLP enzymology, the Cα configuration is strictly controlled by a conserved lysine-mediated protonation mechanism. Thus, mechanisms leading to this α-stereochemistry reversal during the protonation step in radical coupling reactions remains a key question to be elucidated. Furthermore, the stereoselectivity in our previously reported β-dehydroxylative coupling displayed an unusually strong pH dependence, which is rarely observed in traditional closed-shell PLP enzymology. We were intrigued as to whether we could gain further mechanistic understandings on the unusual Cα stereochemistry reversal. In addition, we questioned whether we could evolve next-generation PLP radical enzymes using our previously reported L-*Pf*PLP$^{\beta}$ and D-*Pf*PLP$^{\beta}$ to allow for further enhanced enantiocontrol across a broader pH window. Furthermore, the engineering of PLP radical enzymes with enhanced enantiocontrol may provide additional mechanistic insights into the unusual enantiodivergent protonation mechanism. In this article, we present directed evolution of β-radical PLP enzymes under photobiocatalytic conditions to furnish significantly enhanced stereocontrol and activity. Our studies shed light on the origin of enantioselectivity reversal, suggesting an unusual proton donor switch mechanism, which is rarely observed in conventional two-electron PLP enzymology.

Results and discussion

We recently reported a photobiocatalytic β-dehydroxylative C–C coupling of serine and benzyltrifluoroborate salts using engineered tryptophan synthase β-subunit variants.[48] Our further studies revealed an unusually strong pH dependence of reaction enantioselectivity using both the L-amino acid synthase L-*Pf*PLP$^{\beta}$ and the D-amino acid synthase D-*Pf*PLP$^{\beta}$ (L-*Pf*PLP$^{\beta}$ E104G).

Table 1. Unusual pH Effect on Photobiocatalytic Dehydroxylative C–C Coupling [a]

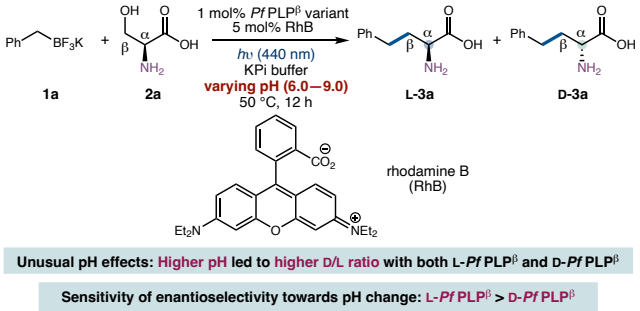

entry	enzyme variant	pH	yield (%)	e.r. (L-**3**:D-**3**)
1	L-*Pf*PLP$^{\beta}$	6.0	73	93:7
2		7.0	76	75:25
3		8.0	71	49:51
4		9.0	66	38:62
5	D-*Pf*PLP$^{\beta}$ (L-*Pf*PLP$^{\beta}$ E104G)	6.0	74	11:89
6		7.0	79	6:94
7		8.0	73	5:95
8		9.0	65	4:96

[a]Reaction conditions: **1** (4.0 mM), **2a** (12.0 mM), 1.0 mol% *Pf*PLP$^{\beta}$, 5 mol% RhB, *hν* (440 nm, 1 W), 200 mM KPi buffer (pH varied) with DMSO (6% v/v) as co-solvent, 50 °C, 10 h.

As can be seen from Table 1, our previously reported PLP radical enzyme L-*Pf*PLP$^{\beta}$ furnished excellent enantioselectivity under acidic conditions. At pH 6.0, the homophenylalanine product **L-3a** formed

in 73% yield and 93:7 e.r. in favor of the L-enantiomer (Table 1, entry 1). As the pH of the reaction medium increased, markedly lower enantioselectivity was observed. For example, at pH 7.0, the e.r. of **3a** decreased to 75:25 (entry 2). At pH 8, **3a** formed in an almost racemic manner (entry 3, 71% yield and 49:51 e.r.). As the pH further increased, L-*Pf*PLP$^{\beta}$ started to show a small preference for **D-3** (entry 4, 66% yield and 38:62 e.r.). With D-*Pf*PLP$^{\beta}$, optimal enantioselectivity was observed under basic conditions and the change of enantiomeric ratio as a function of pH was not as drastic as that with L-*Pf*PLP$^{\beta}$. Specifically, at pH 6.0, homophenylalanine **D-3** formed in 74% yield and 11:89 e.r. (entry 5). As the pH increased from 6.0 to 7.0, 8.0 and 9.0, the e.r. of **D-3a** improved to 6:94, 5:95 and 4:96, respectively (entries 6–8).

Based on these results, as the pH increases, both the L-amino acid synthase L-*Pf*PLP$^{\beta}$ and the D-amino acid synthase D-*Pf*PLP$^{\beta}$ showed a stronger preference for the D-enantiomeric product **D-3a**, as evidenced by a higher **D-3a**/**L-3a** ratio. L-*Pf*PLP$^{\beta}$ exhibited a higher degree of pH sensitivity than D-*Pf*PLP$^{\beta}$. The significant pH dependence of L-*Pf*PLP$^{\beta}$'s enantioselectivity on pH presented a mechanistic conundrum, and the modest degree of enantiocontrol with this previously reported PLP radical enzyme prompted us to further improve its enantioselectivity through directed evolution. Currently, the directed evolution of photobiocatalytic functions involving dual catalytic cycles has remained underdeveloped. Based on previous studies,[41, 49, 50, 54] we further optimized a high-throughput experimental workflow. We developed a mild and high-throughput cell lysis protocol using a 24-tip horn sonicator which is compatible with a broad range of enzymes (see the SI for details). The ability to circumvent the use of lysozyme and other additives that tended to form insoluble precipitates under photobiocatalytic conditions enhanced light absorption and led to improved yields and reproducibility. We further used commercially available 96-position photoreactor with adjustable light intensity for biocatalytic reactions in a 96-well format. The employment of this optimized experimental setup proved to be critical to the success of directed evolution for photobiocatalytic dehydroxylative coupling. The screening of L-*Pf*PLP$^{\beta}$ variants was successfully carried out using cell-free lysates in 96-position photoreactors.

Table 2. Directed Evolution of Second-Generation L-Amino Acid Synthase L-*Pf*PLP$^{\beta\ 2.0}$ [a]

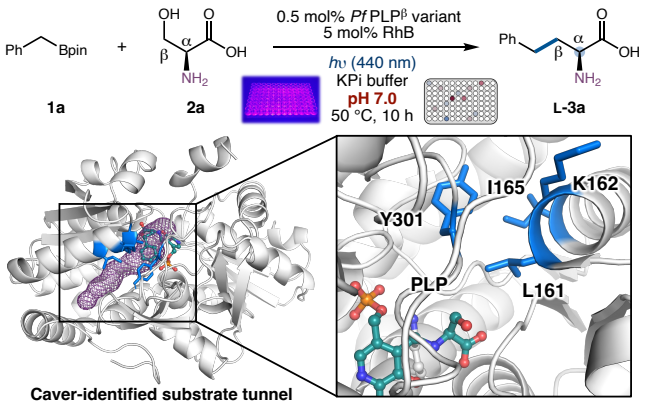

entry	enzyme variant	pH	yield (%)	e.r. (L-**3**:D-**3**)
1	L-*Pf*PLP$^{\beta}$	7.0	57	75:25
2[b]	L-*Pf*PLP$^{\beta}$	7.0	56	75:25
3	L-*Pf*PLP$^{\beta}$ (0.1 mol%)	7.0	16	75:25
4	L-*Pf*PLP$^{\beta}$ Y301H	7.0	76	74:26
5	L-*Pf*PLP$^{\beta}$ Y301H (0.1 mol%)	7.0	52	74:26
6	L-*Pf*PLP$^{\beta}$ Y301H L161M	7.0	73	89:11
7	L-*Pf*PLP$^{\beta}$ Y301H L161M I165L	7.0	65	92:8
8	L-*Pf*PLP$^{\beta}$ Y301H L161M I165L K162F (L-*Pf*PLP$^{\beta\ 2.0}$)	7.0	70	96:4

[a]Reaction conditions: **1a** (4.0 mM), **2a** (12.0 mM), 0.5 mol% L-*Pf*PLP$^{\beta}$, 5 mol% RhB, *h*ν (440 nm, 1 W), 200 mM KPi buffer (pH = 7.0), with DMSO (6% v/v) as the co-solvent, 50 °C, 10 h; [b]Benzyltrifluoroborate salt **1a'** was used as the substrate in lieu of **1a**.

In this study, it was found that benzyl pinacol boronic ester **1a** and benzyltrifluoroborate salt **1a'** exhibited nearly identical yield and enantioselectivity under our photobiocatalytic conditions (Table 2, entries 1 and 2, see Table 7 (*vide infra*) for further discussions). Given that benzyltrifluoroborate salts are usually synthesized from their corresponding pinacol boronates,[80] pinacol boronic ester **1a** and serine **2a** were selected as the model substrates for further optimization. At neutral pH (7.0), we initiated a directed evolution campaign using site-saturation mutagenesis and screening by targeting active-site residues of tryptophan synthase β subunits.[66, 72, 73] This active-site engineering via saturation mutagenesis we undertook herein represented a less explored strategy for the directed evolution of tryptophan synthases.

We first used AutoDock to build a structural model for the homophenylalanine-based external aldimine (**VII** in Scheme 1). Selected active-site residues within 4.0 Å of this PLP covalent intermediate were targeted for SSM. Given the deeply buried active-site of L-*Pf*PLP$^{\beta}$ and the potential importance of substrate tunnel in controlling enzyme activity, we further used Caver[81] to assist in the identification of residues on the substrate tunnel (Table 2). In each round of screening, four active-site residues were randomized by SSM using the 22-codon trick method.[82] 88 clones were chosen per library for screening. In the first round of directed evolution, Y301H was identified as a key beneficial mutation, providing improved yield at reduced enzyme loadings. For example, at a 0.1 mol% biocatalyst loading, with L-*Pf*PLP$^{\beta}$ Y301H, the yield of **3a** improved from 16% to 52% with almost identical enantioselectivity (entries 3 and 5). Starting from L-*Pf*PLP$^{\beta}$ Y301H, an additional three rounds of SSM and screening were carried out, with a focus on residues 161–165 in the α-helix that defines the substrate tunnel of the enzyme. Mutations L161M, I165L, and K162F were found to further enhance the enantioselectivity of the enzyme at neutral pH. Specifically, at pH 7.0, the double mutant L-*Pf*PLP$^{\beta}$ Y301H L161M and triple mutant L-*Pf*PLP$^{\beta}$ Y301H L161M I165L provided **3a** in 89:11 e.r. and 92:8 e.r., respectively (entries 6 and 7). The final variant, L-*Pf*PLP$^{\beta}$ Y301H L161M I165L K162F, which we named as L-*Pf*PLP$^{\beta\ 2.0}$ (second-generation β-radical PLP enzyme), afforded **3a** in 96:4 e.r. (entry 8).

Table 3. Second-Generation Enzyme L-*Pf*PLP$^{\beta\ 2.0}$ Displayed Enhanced Enantiocontrol Across a Broader pH Window [a]

https://doi.org/10.26434/chemrxiv-2025-32vjk **ORCID:** https://orcid.org/0000-0002-2473-6827

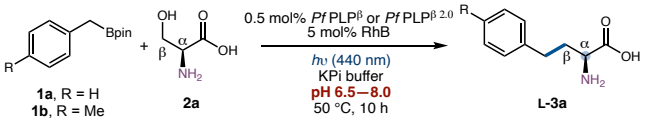

entry	substrate	enzyme variant	pH	yield (%)	e.r. (L-**3**:D-**3**)
1	**1a**	L-*Pf*PLP$^{\beta\ 2.0}$	6.5	54	97:3
2	**1a**	L-*Pf*PLP$^{\beta\ 2.0}$	7.0	70	96:4
3	**1a**	L-*Pf*PLP$^{\beta\ 2.0}$	7.5	62	92:8
4	**1a**	L-*Pf*PLP$^{\beta\ 2.0}$	8.0	60	84:16
5	**1b**	L-*Pf*PLP$^{\beta\ 2.0}$	7.0	81	99:1
6	**1b**	L-*Pf*PLP$^{\beta}$	7.0	78	35:65
7	**1b**	L-*Pf*PLP$^{\beta\ 2.0}$ (0.1 mol%)	7.0	53	99:1
8	**1b**	L-*Pf*PLP$^{\beta}$ (0.1 mol%)	7.0	42	35:65

[a]Reaction conditions: **1a** (4.0 mM), **2a** (12.0 mM), 0.5 mol% L-*Pf*PLP$^{\beta}$, 5 mol% RhB, *hν* (440 nm, 1 W), 200 mM KPi buffer (pH), with DMSO (6% v/v) as the co-solvent, 50 °C, 10 h.

Moreover, L-*Pf*PLP$^{\beta\ 2.0}$ provided consistently improved enantioselectivity across the pH window relative to the first-generation enzyme (Table 3). For example, at pH 8, this second-generation radical PLP enzyme L-*Pf*PLP$^{\beta\ 2.0}$ still catalyzed the formation of **3a** in 84:16 e.r. (Table 3, entry 4). In contrast, at this pH, our previously reported first-generation enzyme L-*Pf*PLP$^{\beta}$ led to **3a** in 49:51 e.r. (Table 1, entry 3). Furthermore, L-*Pf*PLP$^{\beta\ 2.0}$ also exhibited improved performance when *para*-methyl-substituted benzylboronic acid pinacol ester (**1b**) was employed as the substrate, providing the radical C–C coupling product **3b** in 81% yield and 99:1 e.r. at pH 7.0 (Table 3, entry 5). By contrast, under these conditions, the use of first-generation enzyme L-*Pf*PLP$^{\beta}$ led to 35:65 e.r. favoring **D-3b** (entry 6). With a further decreased biocatalyst loading of 0.1 mol%, L-**3b** formed in 53% yield and 99:1 e.r. (entry 7), indicating improved catalytic efficiency of the second-generation enzyme relative to the first-generation enzyme (entry 8). Additionally, *meta*- and *ortho*-substituted substrates **1c** and **1d** displayed different requirement for the biocatalyst. L-*Pf*PLP$^{\beta}$ L161A K162V (L-*Pf*PLP$^{\beta\ 2.0b}$) was engineered to provide enhanced enantiocontrol (see SI table S7 for details).

Table 4. Development of Second-Generation D-Amino Acid Synthase D-*Pf*PLP$^{\beta\ 2.0}$ [a]

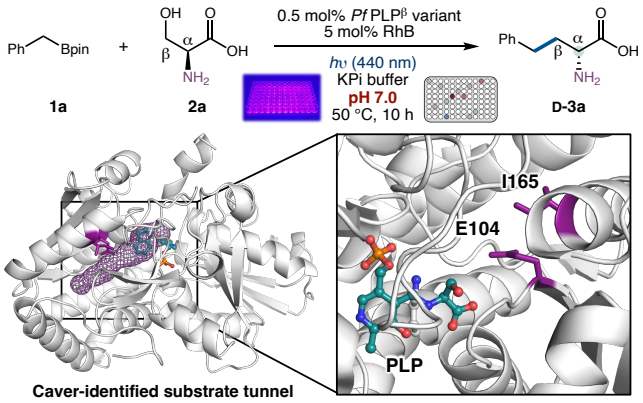

entry	enzyme variant	pH	yield (%)	e.r. (L-**3**:D-**3**)
1	D-*Pf*PLP$^{\beta}$	7.5	67	6:94
2	D-*Pf*PLP$^{\beta}$ G104P (D-*Pf*PLP$^{\beta\ 2.0}$)	7.5	77	3:97
3	D-*Pf*PLP$^{\beta}$ (0.1 mol%)	7.5	17	6:94
4	D-*Pf*PLP$^{\beta\ 2.0}$ (0.1 mol%)	7.5	33	3:97
5	D-*Pf*PLP$^{\beta\ 2.0}$	6.5	70	5:95
6	D-*Pf*PLP$^{\beta\ 2.0}$	7.0	75	4:96
7	D-*Pf*PLP$^{\beta\ 2.0}$	8.0	74	3:97

[a]Reaction conditions: **1a** (4.0 mM), **2a** (12.0 mM), 0.5 mol% D-*Pf*PLP$^{\beta}$, 5 mol% RhB, *hν* (440 nm, 0.11 W), 200 mM KPi buffer (pH = 7.5), DMSO (6% v/v), 50 °C, 10 h.

Similarly, the activity and enantioselectivity of the D-amino acid synthase D-*Pf*PLP$^{\beta}$ could also be improved by protein engineering (Table 4). Assisted by our active-site and tunnel models, site-saturation mutagenesis and screening led to D-*Pf*PLP$^{\beta}$ G104P as a further improved variant with both higher activity and enantioselectivity. At pH 7.5 and 0.5 mol% loading of *Pf*PLP$^{\beta}$ G104P, D-**3a** formed in 77% yield and 3:97 e.r. (Table 4, entry 2). Under these conditions, D-*Pf*PLP$^{\beta}$ provided D-**3a** in 67% yield and 6:94 e.r. (entry 1). At a further reduced enzyme loading of 0.1 mol%, D-*Pf*PLP$^{\beta}$ G104P still afforded D-**3a** in 33% yield and 3: 97 e.r. (entry 4). By contrast, the first-generation enzyme D-*Pf*PLP$^{\beta}$ only delivered in 17% yield and 6:94 e.r. under identical conditions (entry 3). We named D-*Pf*PLP$^{\beta}$ G104P as D-*Pf*PLP$^{\beta\ 2.0}$. Across a pH window ranging from 6.5 to 8.0, D-*Pf*PLP$^{\beta\ 2.0}$ exhibited minimal variation in enantioselectivity (5:95 e.r. at pH 6.5, 4:96 e.r. at pH 7.0, and 3:97 e.r. at pH 8.0, entries 4–7). At these pHs, the enantioselectivity of D-*Pf*PLP$^{\beta\ 2.0}$ was found to be consistently better than the first-generation enzyme D-*Pf*PLP$^{\beta}$.

Notably, in this enzyme engineering study, in addition to E104G and E104P, several other single mutations were discovered to reverse the enantiopreference of L-*Pf*PLP$^{\beta}$. Residue 165 which is spatially close to residue 104 was found to exert a critical role in the enzymatic enantiocontrol. Replacing the large hydrophobic isoleucine (I) at 165 with a smaller alanine or glycine, the enzyme variants showed inverted enantiopreference. L-*Pf*PLP$^{\beta}$ I165A exhibited an e.r. of 9:91 in favor of D-**3a** (Table 5, entry 3), while L-*Pf*PLP$^{\beta}$ I165G

showed an e.r. of 7:93 for D-**3a** (entry 4). Replacing I165 with a hydrophilic side chain serine (I165S) also resulted in enantioselectivity switch to favor D-**3a** (8:92 e.r., entry 5). The discovery of additional single mutations leading to enantiopreference reversal bears broad implications in the enzymatic protonation mechanism. Further combination of the E104P mutation of D-*Pf*PLP$^{\beta\ 2.0}$ and these I165X mutations did not afford further enhanced enantiocontrol. Therefore, D-*Pf*PLP$^{\beta\ 2.0}$ was used for further substrate scope examination and mechanistic studies.

Table 5. Discovery of New Stereoinvertive D-Amino Acid Synthase Variants[a]

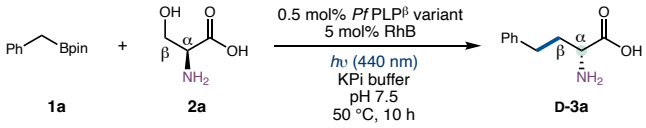

1a **2a** **D-3a**

entry	enzyme variant	yield (%)	e.r. (L-**3**:D-**3**)
1	D-*Pf*PLP$^{\beta}$ (L-*Pf*PLP$^{\beta}$ E104G)	67	6:94
2	D-*Pf*PLP$^{\beta\ 2.0}$ (L-*Pf*PLP$^{\beta}$ E104P)	77	3:97
3	L-*Pf*PLP$^{\beta}$ I165A	54	9:91
4	L-*Pf*PLP$^{\beta}$ I165G	47	7:93
5	L-*Pf*PLP$^{\beta}$ I165S	36	8:92

[a]Reaction conditions: **1a** (4.0 mM), **2a** (12.0 mM), 0.5 mol% *Pf*PLP$^{\beta}$ variant, 5 mol% RhB, *hν* (440 nm, 0.11 W), 200 mM KPi buffer (pH = 7.5), DMSO (6% v/v), 50 °C, 10 h.

With a set of second-generation enantiodivergent PLP radical enzymes in hand, we set out to explore the substrate scope of this photobiocatalytic asymmetric dehydroxylative C–C coupling (Table 6). Both second-generation enzyme variants L-*Pf*PLP$^{\beta\ 2.0}$ and D-*Pf*PLP$^{\beta\ 2.0}$ were found to effectively facilitate the biotransformation of a wide range of organoboronate substrates. For substrates possessing a *para*-substituent (**3b** and **3e**–**3j**) or an *ortho*- (**3d** and **3o**) substituents on the aromatic ring, first-generation enzyme L-*Pf*PLP$^{\beta}$ produced the undesired D-amino acid with low enantioselectivity. In contrast, with L-*Pf*PLP$^{\beta\ 2.0}$ and L-*Pf*PLP$^{\beta\ 2.0b}$, substituted organoboronate substrates were converted into L-amino acids with good yields (up to 89%) and excellent enantioselectivity (up to >99:1 e.r.). Substrates with an electron-donating *para*-substituent such as methyl (**3b**), methoxy (**3e**), and methylthio (**3f**) were converted with excellent yield and enantiocontrol. Halogen substituents including a fluorine (**3g**), a chlorine (**3h**), and a bromine (**3i**) were well-tolerated. Benzylboronates bearing a large *para*-phenyl group (**3j**) were also accepted, further showcasing the promiscuity of this enzyme. Using L-*Pf*PLP$^{\beta\ 2.0b}$, *meta*- (**3c** and **3k**–**3n**) and *ortho*-substituted (**3d** and **3o**–**3p**) organoboronate substrates could be successfully also converted into the corresponding ncAAs with good yields (up to 84%) and enantioselectivities (up to 95:5 e.r.). Substrates bearing an electron-withdrawing group, such as a cyano (**3m**) and a trifluoromethyl (**3n**), were found to be compatible. Importantly, using commercially available blue LED lamps, this photobiocatalytic amino acid synthesis could be scaled up conveniently. At a 0.8-mmol scale, over 100 mg of L-**3b** could be prepared in one batch with excellent enantioselectivity (60% yield, 110 mg, 99:1 e.r.), illustrating the potential application of this enzyme technology in a medicinal chemistry setting.

When D-*Pf*PLP$^{\beta\ 2.0}$ was applied, substrates with a *para*-, a *meta*-, or an *ortho*-substituent were transformed with good yield and enantioselectivity (D-**3a**–D-**3p**). A broad range of C–C coupling products formed with consistently good enantioselectivity (up to 1:99 e.r.). For D-**3o**, a slight decrease in enantioselectivity (31% yield, 11:89 e.r.) was observed presumably due to the presence of a larger chlorine substituent.

In the present study, we developed photobiocatalytic protocols for the transformation of benzylboronic acid pinacol esters. Compared to our previous report based on the use of benzyltrifluoroborate salts, the ability to transform easily accessible pinacol boronic esters further enhanced the applicability of the process. To systematically assess the utility of a wider range of organoboron reagents, we examined benzylboronic acid pinacol ester (**1a**), benzyltrifluoroborate (**1a'**),[80] benzylboronic acid (**1a''**) and benzyl *N*-methyliminodiacetyl (MIDA)[83, 84] boronate (**1a'''**) with our second-generation biocatalyst L-*Pf*PLP$^{\beta\ 2.0}$. It was found that **1a**, **1a'** and **1a''** exhibited almost identical activity under the standard conditions with our evolved enzyme L-*Pf*PLP$^{\beta\ 2.0}$ (Table 7). By contrast, the use of MIDA boronate **1a'''** did not lead to the formation of **3a**.

Table 6. Enantiodivergent Photobiocatalytic C–C Coupling of Organoboronic Acid Pinacol Esters Using Second-Generation PLP Enzymes: Substrate Scope [a]

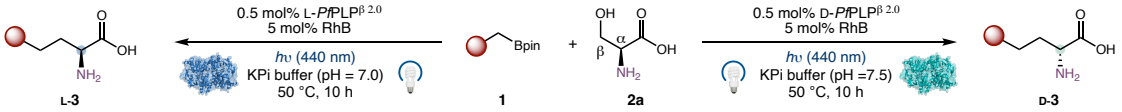

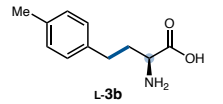

L-3b
(81 ± 1)% (77%)[b] yield, 99:1 e.r.
[110 mg scale] 60% yield, 99:1 e.r.

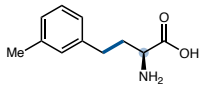

L-3c
(64 ± 2)% yield, 93:7 e.r.[c]

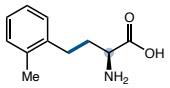

L-3d
(67 ± 1)% yield, 89:11 e.r.[c]

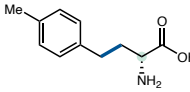

D-3b
(86 ± 2)% yield, 1:99 e.r.

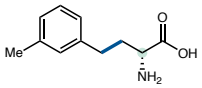

D-3c
(66 ± 4)% yield, 3:97 e.r.

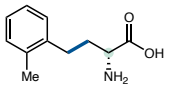

D-3d
(73 ± 3)% yield, 4:96 e.r.

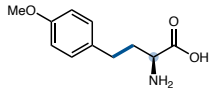

L-3e
(82 ± 3)% yield, 94:6 e.r.
L-*Pf*PLPβ: 80% yield, 12:88 e.r.

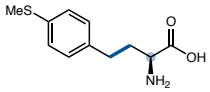

L-3f
(89 ± 1)% yield, 98:2 e.r.
L-*Pf*PLPβ: 67% yield, 12:88 e.r.

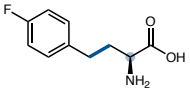

L-3g
(89 ± 2)% yield, 91:9 e.r.
L-*Pf*PLPβ: 44% yield, 43:57 e.r.

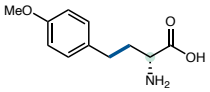

D-3e
(88 ± 2)% yield, 1:99 e.r.

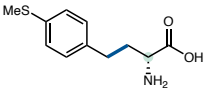

D-3f
(73 ± 3)% yield, 4:96 e.r.

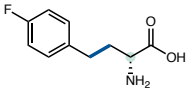

D-3g
(91 ± 2)% yield, 1:99 e.r.

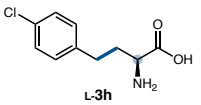

L-3h
(84 ± 4)% yield, 97:3 e.r.
L-*Pf*PLPβ: 77% yield, 20:80 e.r.

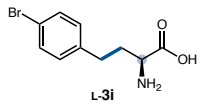

L-3i
(69 ± 2)% yield, 97:3 e.r.
L-*Pf*PLPβ: 62% yield, 15:85 e.r.

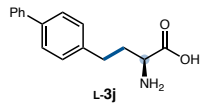

L-3j
(88 ± 6)% yield, 89:11 e.r.
L-*Pf*PLPβ: 90% yield, 21:79 e.r.

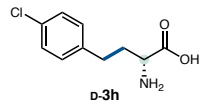

D-3h
(72 ± 2)% yield, 1:99 e.r.

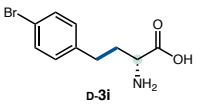

D-3i
(51 ± 3)% yield, 1:99 e.r.

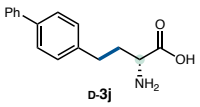

D-3j
(40 ± 1)% yield, 6:94 e.r.

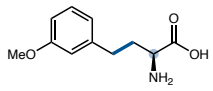

L-3k
(70 ± 4)% yield, 94:6 e.r.

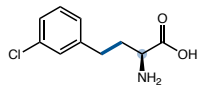

L-3l
(71 ± 5)% yield, 95:5 e.r.

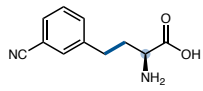

L-3m
(40 ± 3)% yield, 93:7 e.r.

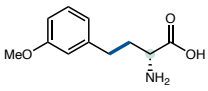

D-3k
(83 ± 2)% yield, 2:98 e.r.

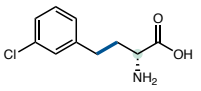

D-3l
(52 ± 1)% yield, 4:96 e.r.

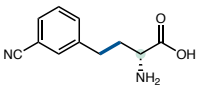

D-3m
(54 ± 1)% yield, 2: 98 e.r.

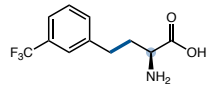

L-3n
(33 ± 2)% yield, 94:6 e.r.[d]

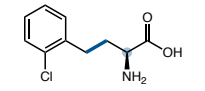

L-3o
(74 ± 5)% yield, 92:8 e.r.[d]

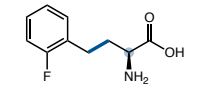

L-3p
(84 ± 1)% yield, 94:6 e.r.[d]

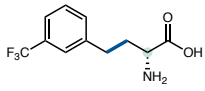

D-3n
(36 ± 1)% yield, 3: 97 e.r.

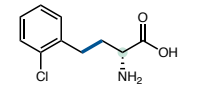

D-3o
(31 ± 2)% yield, 11:89 e.r.

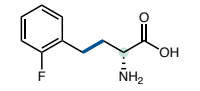

D-3p
(79 ± 2)% yield, 4: 96 e.r.

[a]Reaction conditions for L-amino acid synthesis: **1** (4.0 mM), **2a** (12.0 mM), 0.5 mol% L-*Pf*PLP$^{\beta\ 2.0}$, 5 mol% RhB, *hν* (440 nm, 1 W), 200 mM KPi buffer (pH = 7.0), DMSO (6% v/v), 50 °C, 10 h. Reaction conditions for D-amino acid synthesis: **1** (4.0 mM), **2a** (12.0 mM), 0.5 mol% D-*Pf*PLP$^{\beta\ 2.0}$, 5 mol% RhB, *hν* (440 nm, 0.11 W), 200 mM KPi buffer (pH = 7.5), DMSO (6% v/v), 50 °C, 10 h. [b]Isolated yield on a 0.10 mmol scale. [c]Isolated yield on a 110 mg scale. [d]1.0 mol% L-*Pf*PLP$^{\beta\ 2.0b}$ was used as in lieu of L-*Pf*PLP$^{\beta\ 2.0}$.

Table 7. Use of Other Organoboron Species for Photobiocatalytic Coupling [a]

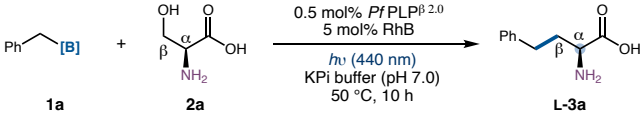

1a **2a** **L-3a**

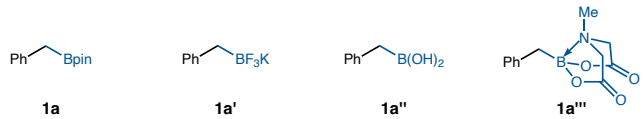

1a **1a'** **1a"** **1a'''**

entry	1	yield (%)	e.r.
1	**1a**	70	96:4
2	**1a'**	69	96:4
3	**1a"**	63	96:4
4	**1a'''**	0	-

[a]Reaction conditions: **1** (4.0 mM), **2a** (12.0 mM), 0.5 mol% L-*Pf*PLP$^{\beta\ 2.0}$, 5 mol% RhB, *hν* (440 nm, 1 W), 200 mM KPi buffer (pH = 7.0) with DMSO (6% v/v) as the co-solvent, 50 °C, 10 h.

To further understand the resting state of these organoboron reagents in the aqueous KPi buffer, ^{11}B and ^{1}H NMR spectroscopic analysis was carried out (Scheme 2). In ^{11}B NMR, benzyltrifluoroborate **1a'** showed a characteristic signal at 3.8 ppm while benzylboronic acid **1a"** and benzylboronic acid pinacol ester **1a** displayed similar chemical shifts at ca. 32 ppm. Benzylboronic acid **1a"** and benzylboronic acid pinacol ester **1a** could be conveniently resolved in ^{1}H NMR using their benzylic proton signals (2.16 and 2.07 ppm in DMSO-d_6, respectively). ^{11}B NMR spectroscopy revealed that in KPi buffer, benzyltrifluoroborate **1a'** rapidly and completely hydrolyzed to benzylboronic acid **1a"**. This finding is in line with previous study on the stability of these reagents in Suzuki coupling reactions.[85] In contrast, ^{1}H NMR spectroscopic analysis showed that in KPi buffer (pH 7.0) at 50 °C, benzylboronic acid pinacol ester **1a** established an equilibrium with benzylboronic acid **1a"** in ca. 30 min. When this equilibrium was fully established, the **1a**:**1a"** ratio was ca. 53:47. These results showed that the free benzylboronic acid **1a"** is likely a common radical precursor under photobiocatalytic conditions when benzyltrifluoroborate **1a'** and benzylboronic acid pinacol ester **1a** are used. Under these conditions, ^{11}B signal corresponding to the ate complex [R-B(OH)$_3^-$] was not observed, both at room temperature and after heat treatment at 50 °C or with increased concentrations. Although this ate complex was not observed, based on previous studies, [86,87] we hypothesized that the formation of a transient hydroxy ate complex [R-B(OH)$_3^-$] or aqua complex [R-B(OH)$_2$(H$_2$O)] of the benzylboronic acid substantially lowered its single-electron oxidation potential, thus facilitating radical generation. In previously developed synthetic transformations using

organic solvents, the use of Lewis base additives such as DMAP was found to be critical in facilitating the single-electron oxidation of organoboron reagents under photoredox conditions.[88, 89] The accelerated radical formation from organoboron reagents in aqueous buffer without introducing Lewis base additives represented a key feature in our photobiocatalytic radical transformations involving organoboron substrates.

Scheme 2. ^{11}B and ^{1}H NMR Spectroscopic Analysis Showed Rapid *In Situ* Hydrolysis of Trifluoroborates and Pinacol Boronic Esters in KPi Buffer

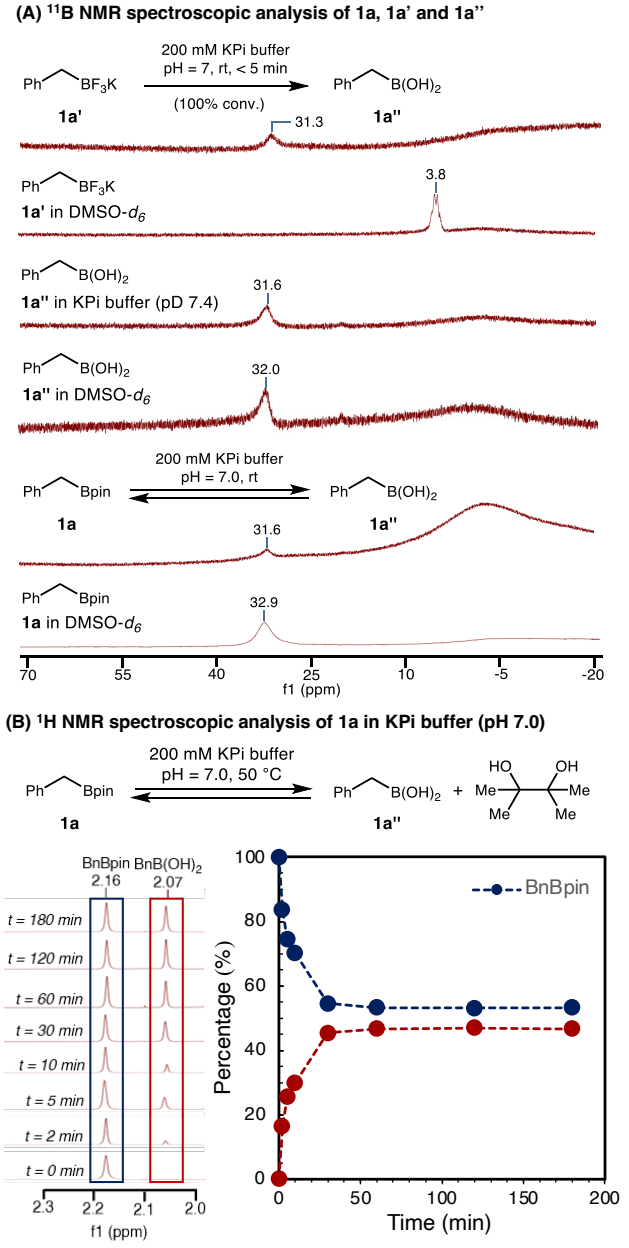

With these improved second-generation PLP biocatalysts, we further investigated the origin of enantioselectivity reversal in D-*Pf*PLP$^{\beta}$-catalyzed β-dehydroxylative radical C–C coupling. First, we carried out studies to probe whether this enantioselectivity reversal also occurs in the native closed-shell tryptophan synthesis activity (see SI Table S17 for details). It was found that in the native tryptophan synthase activity, all the enzymes resulting from the present study, including L-*Pf*PLP$^{\beta}$, L-*Pf*PLP$^{\beta\ 2.0}$, D-*Pf*PLP$^{\beta}$ and D-*Pf*PLP$^{\beta\ 2.0}$ favored the formation of natural L-tryptophan (L-**5**). With D-*Pf*PLP$^{\beta\ 2.0}$, trace amount of D-tryptophan (D-**5**) was observed (97:3 e.r.). The high enantiopreference for L-tryptophan of all the engineered PLP enzymes is consistent with the canonical understanding that the α-stereochemistry of amino acid products in this closed-shell process is dictated by reprotonation via a conserved lysine residue. Thus, the unusual absolute stereochemical reversal is unique to the photobiocatalytic radical coupling, indicating a new mechanism in the enantioselective protonation step.

Furthermore, we discovered an unexpected racemization of homophenylalanine product L-**3a** catalyzed by engineered PLP enzymes. As shown in Table 8, in the presence of our first-generation enzyme L-*Pf*PLP$^{\beta}$, at 50 °C and pH 8.0, optically pure L-**3a** (>99:1 e.r.) underwent complete racemization after 24 h (entry 1). Control experiments showed that this racemization is enabled by the enzyme L-*Pf*PLP$^{\beta}$, as no racemization was observed in the absence of the enzyme (entry 2) or in the presence of free PLP cofactor (entry 3). This racemization is promoted by basic conditions, as carrying out this conversion at pH 7.0 resulted in incomplete racemization after 24 h (entry 4). D-homophenylalanine (D-**3a**) also underwent racemization in the presence of first-generation enzyme L-*Pf*PLP$^{\beta}$ despite a slower racemization rate (40:60 e.r.) after 24 h in the presence of L-*Pf*PLP$^{\beta}$, entry 6). These results showed that our first-generation radical PLP enzyme L-*Pf*PLP$^{\beta}$ can bind either L- or D-homophenylalanine and induce racemization in a way reminiscent of PLP-dependent amino acid.[90-93] We postulated that this racemase activity is due to the presence of an alternative proton donor from the opposite face of the PLP covalent intermediate.

Table 8. Unexpected Promiscuous Racemase Activity of L-Amino Acid Synthase L-*Pf*PLP$^{\beta}$ [a]

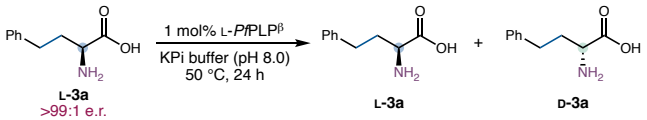

entry	variation from the standard	e.r. (L-:D-)
1	none	50:50
2	No enzyme	>99:1
3	No enzyme, 10 mol% PLP	>99:1
4	pH = 7.0	80:20
5	pH = 9.0	50:50
6	D-**3a** (<1:99 e.r.) instead of L-**3a**	40:60
7	L-*Pf*PLP$^{\beta}$ Y301H	92:8
8	L-*Pf*PLP$^{\beta}$ Y301H L161M	95:5
9	L-*Pf*PLP$^{\beta}$ Y301H L161M I165L	98:2
10	L-*Pf*PLP$^{\beta}$ Y301H L161M I165L K162F (L-*Pf*PLP$^{\beta\ 2.0}$)	98:2 (99:1)[b]

[a]Reaction conditions: **L-3a** (4.0 mM) 1.0 mol% L-*Pf*PLP$^{\beta}$, 200 mM KPi buffer (pH = 8.0) with DMSO (10% v/v) as the co-solvent, 50 °C, 24 h. [b]Reaction was carried out at pH 7.0 instead of pH 8.0.

We further investigated whether this enzymatic racemization is still operative with our L-*Pf*PLP$^{\beta\ 2.0}$ evolutionary lineage (Table 8,

entries 7–10). Importantly, these studies showed that evolved L-*Pf*PLP$^{\beta}$ variants nearly abolished this unexpected promiscuous racemase activity. As can be seen from entry 7, the Y301H mutation played the most important role in suppressing this racemization activity, and homophenylalanine **3a** was recovered in 92:8 e.r. after treatment with L-*Pf*PLP$^{\beta}$ Y301H at 50 °C and pH 8.0 for 24 h. The inclusion of additional beneficial mutations including L161M and I165L further reduced this racemization activity (entries 8 and 9). With the final variant L-*Pf*PLP$^{\beta}$ Y301H L161M I165L K162F (L-*Pf*PLP$^{\beta\ 2.0}$), only 2% L-homophenylalanine (L-**3a**) underwent racemization after 24 h (entry 10). At pH 7, almost no racemization of L-**3a** was observed with L-*Pf*PLP$^{\beta\ 2.0}$ (entry 10). Collectively, these results showed that evolved second-generation enzyme L-*Pf*PLP$^{\beta\ 2.0}$ allowed for enhanced enantiocontrol, in part due to the abolishment of this promiscuous racemase activity.

We propose that the enantiodivergent protonation in our engineered radical PLP enzymes may stem from the switch of proton donors (Scheme 3). We posit that the racemization process of L-**3a** involves substrate binding and subsequent formation of an external aldimine with the PLP enzyme. Enzymatic deprotonation with the conserved lysine residue would lead to a quinonoid intermediate. Starting from this quinonoid, reprotonation by the ε-ammonium of the lysine residue from the (*Re*)-face regenerates the same external aldimine, while reprotonation from the opposite side ((*Si*)-face) with water molecules yields a new aldimine with enantioinversion. Furthermore, we postulate that the proton donor water molecules in the active site of our first-generation enzyme L-*Pf*PLP$^{\beta}$ are associated with Y301, resulting in their enhanced acidity. The Y301H mutation attenuates the acidity of active-site water molecules, thereby effectively suppressing this promiscuous racemase activity. Our results with the racemization of D-**3a** indicates that the PLP enzyme can also bind this D-amino acid and trigger racemization.

Scheme 3. Proposed Proton Donor Switch Mechanism to Account for the Promiscuous Racemase Activity

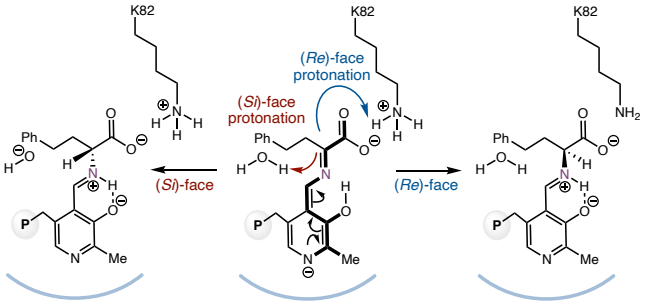

To gain further insights into the protonation mechanism in the dehydroxylative C–C coupling process, deuterium labeling experiments with deuterated solvent D_2O were performed (Table 9). Using the second-generation L-amino acid synthase L-*Pf*PLP$^{\beta\ 2.0}$, α-deuterated L-**3a** was produced as confirmed by HPLC-MS analysis. With L-*Pf*PLP$^{\beta\ 2.0}$, as the pD of the KPi buffer increased from 6.4 to 7.4, the yield of L-**3a** increased from 33% (Table 9, entry 1) to 61% (entry 2). As pD further increased to 8.4, the yield of L-**3a** decreased to 55% (entry 3). The enantioselectivity of *Pf*PLP$^{\beta\ 2.0}$ progressively decreased from 99:1 e.r. (entry 1) to 98:2 e.r. (entry 2) to 91:9 e.r. (entry 3), as the pD increased. Overall, the trends in yield and selectivity mirrored those observed with the pH effects with H_2O-based buffer (Table 9, entries 1–3 in the parentheses). Importantly, when the reaction medium was changed from H_2O to D_2O, further enhancement of the enantiomeric purity of the L-homophenylalanine product (L-**3a**) was observed, suggesting the production of D-**3a** is slower in D_2O.

When the second-generation enzyme D-*Pf*PLP$^{\beta\ 2.0}$ was used, α-deuterated D-**3a** formed using D_2O based buffer. Our HPLC-MS analysis showed that the degree of deuterium incorporation was >90%. With D-*Pf*PLP$^{\beta\ 2.0}$, relative to photobiocatalytic reactions carried out with a H_2O-based medium, a notable decrease of the yield of the D-homophenylalanine product (D-**3a**) was observed (25–30%) across the investigated pD range (6.4–8.4) (Table 9, entries 4–6). Furthermore, the e.r. of D-**3a** with D_2O was found to be much lower than those results with H_2O (entries 4–6 in the parentheses). Consistent with our results with L-*Pf*PLP$^{\beta\ 2.0}$, these studies also showed that the production of D-**3a** is slower in D_2O when D-*Pf*PLP$^{\beta\ 2.0}$ was used.

Table 9. Photobiocatalytic C–C Coupling in D_2O buffer: Effects on Yield and Enantioselectivity [a]

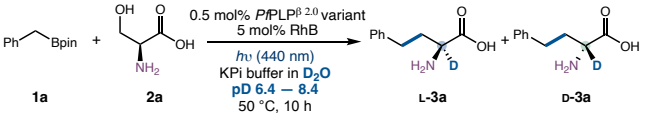

1a **2a** **L-3a** **D-3a**

entry	*Pf*PLP$^{\beta}$ variants	pD	yield (%)	e.r. (L-**3**:D-**3**)
1	L-*Pf*PLP$^{\beta\ 2.0}$	6.4	33 (19)[b]	99:1 (99:1)[b]
2	L-*Pf*PLP$^{\beta\ 2.0}$	7.4	61 (70)[b]	98:2 (96:4)[b]
3	L-*Pf*PLP$^{\beta\ 2.0}$	8.4	55 (60)[b]	91:9 (84:16)[b]
4	D-*Pf*PLP$^{\beta\ 2.0}$	6.4	26 (66)[b]	17:83 (6:94)[b]
5	D-*Pf*PLP$^{\beta\ 2.0}$	7.4	27 (75)[b]	12:88 (4:96)[b]
6	D-*Pf*PLP$^{\beta\ 2.0}$	8.4	29 (74)[b]	7:93 (3:97)[b]

[a]Reaction conditions: **1a** (4.0 mM), **2a** (12.0 mM), 0.5 mol% L-*Pf*PLP$^{\beta\ 2.0}$ or D-*Pf*PLP$^{\beta\ 2.0}$, 5 mol% RhB, *hv* (440 nm), 200 mM KPi buffer (D_2O) with DMSO (6% v/v) as co-solvent, 50 °C, 10 h, [b]Yields and e.r.'s with the corresponding H_2O-based KPi buffer were reported in parentheses. pH = pD – 0.4.

Taken together, these results suggest that with both the L-amino acid synthase L-*Pf*PLP$^{\beta\ 2.0}$ and the D-amino acid synthase D-*Pf*PLP$^{\beta\ 2.0}$, the unusual D-amino acid forming protonation pathway may involve the solvent water molecule as the promiscuous proton donor (Scheme 3). In the canonical L-amino acid producing pathway, the protonated lysine residue serves as the proton donor as in this two-electron PLP enzymology. In contrast, in the non-canonical D-amino acid producing pathway, water molecules from the opposite site of the lysine residue (*Si*-face) serve as the proton donor, resulting in the enantioselectivity reversal. We note that this non-canonical protonation pathway is likely related to our unexpected findings on the promiscuous racemase activity where protonation can occur from either the (*Re*)-face or the (*Si*)-face.

Additionally, we further analyzed other D-amino acid producing mutants, including the I165A, I165G and I165S mutants (Table 5).

As the substrate tunnel is further broadened with these I165X mutants, a higher amount of water molecules would be present from the other side ((*Si*)-face) of the PLP covalent intermediate opposite to that of the conserved lysine. Thus, these mutants showed a stronger preference for (*Si*)-face reprotonation leading to D-amino acid.

Conclusions

In summary, through high-throughput photobiocatalysis, we have successfully developed second-generation PLP biocatalysts for the enantiodivergent synthesis of non-canonical amino acids via radical dehydroxylative coupling. Both the conventional L- amino acids and the unusual enantiomeric D- amino acids could be prepared from the same L-serine through a rare enzyme controlled stereoretentive or stereoinvertive C–C coupling. The newly engineered enzymes enabled the use of a broad range of organoboron radical precursors to be applied with high enantioselectivity. In particular, *para*- and *ortho*-substituted organoboron substrates showing low levels of enantioselectivity with our previously reported first-generation enzyme could now be transformed with excellent enantiocontrol. Importantly, mechanistic studies on racemization and solvent deuterium effects revealed an unusual proton donor switch mechanism to account for this non-canonical stereoinvertive C–C coupling. Our evolved L- amino acid synthase allowed for much higher enantiocontrol, in part due to the abolishment of the unexpected racemase activity. Equipped with these understandings, ongoing research in our laboratory aims to further engineer PLP biocatalysts for radical biocatalysis, ultimately significantly expanding the toolbox of biocatalytic non-canonical amino acid synthesis.

ASSOCIATED CONTENT

Supporting Information

The Supporting Information is available free of charge on the ACS Publications website.

Experimental procedures, DNA and protein sequences, characterization data, HPLC traces and NMR spectra (PDF).

AUTHOR INFORMATION

Corresponding Author

Yang Yang – *Department of Chemistry and Biochemistry, University of California Santa Barbara, Santa Barbara, California 93106, United States; Biomolecular Science and Engineering Program, University of California Santa Barbara, Santa Barbara, California 93106, United States; orcid.org/0000-0002-4956-2034; Email: yang@chem.ucsb.edu*

Authors

Lei Cheng – Department of Chemistry and Biochemistry, University of California Santa Barbara, Santa Barbara, California 93106, United States; orcid.org/0000-0002-2473-6827

Zhiyu Bo – Department of Chemistry and Biochemistry, University of California Santa Barbara, Santa Barbara, California 93106, United States

Benjamin Krohn-Hansen – Department of Chemistry and Biochemistry, University of California Santa Barbara, Santa Barbara, California 93106, United States

ACKNOWLEDGMENT

We acknowledge the Army Research Office and Army Center for Synthetic Biology for financial support (W911NF-24-2-0246).

REFERENCES

1. Turner, N. J., Directed evolution drives the next generation of biocatalysts. *Nat. Chem. Biol.* **2009,** *5*, 567-573.
2. Bornscheuer, U. T.; Huisman, G. W.; Kazlauskas, R. J.; Lutz, S.; Moore, J. C.; Robins, K., Engineering the third wave of biocatalysis. *Nature* **2012,** *485*, 185-194.
3. Devine, P. N.; Howard, R. M.; Kumar, R.; Thompson, M. P.; Truppo, M. D.; Turner, N. J., Extending the application of biocatalysis to meet the challenges of drug development. *Nat. Rev. Chem.* **2018,** *2*, 409-421.
4. Buller, R.; Lutz, S.; Kazlauskas, R. J.; Snajdrova, R.; Moore, J. C.; Bornscheuer, U. T., From nature to industry: Harnessing enzymes for biocatalysis. *Science* **2023**, *382*, eadh8615.
5. Chen, K.; Arnold, F. H., Engineering new catalytic activities in enzymes. *Nat. Catal.* **2020,** *3*, 203-213.
6. Yang, Y.; Arnold, F. H., Navigating the Unnatural Reaction Space: Directed Evolution of Heme Proteins for Selective Carbene and Nitrene Transfer. *Acc. Chem. Res.* **2021,** *54*, 1209-1225.
7. Brandenberg, O. F.; Fasan, R.; Arnold, F. H., Exploiting and engineering hemoproteins for abiological carbene and nitrene transfer reactions. *Curr. Opin. Biotechnol.* **2017,** *47*, 102-111.
8. Harrison, W.; Huang, X.; Zhao, H., Photobiocatalysis for Abiological Transformations. *Acc. Chem. Res.* **2022,** *55*, 1087-1096.
9. Klaus, C.; Hammer, S. C., New catalytic reactions by enzyme engineering. *Trends in Chemistry* **2022,** *4*, 363-366.
10. Emmanuel, M. A.; Bender, S. G.; Bilodeau, C.; Carceller, J. M.; DeHovitz, J. S.; Fu, H.; Liu, Y.; Nicholls, B. T.; Ouyang, Y.; Page, C. G.; Qiao, T.; Raps, F. C.; Sorigué, D. R.; Sun, S.-Z.; Turek-Herman, J.; Ye, Y.; Rivas-Souchet, A.; Cao, J.; Hyster, T. K., Photobiocatalytic Strategies for Organic Synthesis. *Chem. Rev.* **2023**, 9, 5459–5520.
11. Fu, H.; Hyster, T. K., From Ground-State to Excited-State Activation Modes: Flavin-Dependent "Ene"-Reductases Catalyzed Non-natural Radical Reactions. *Acc. Chem. Res.* **2024**, *57*, 1446–1457.
12. Reisenbauer, J. C.; Sicinski, K. M.; Arnold, F. H., Catalyzing the future: recent advances in chemical synthesis using enzymes. *Curr. Opin. Chem. Biol.* **2024,** *83*, 102536.
13. Sibi, M. P.; Manyem, S.; Zimmerman, J., Enantioselective Radical Processes. *Chem. Rev.* **2003,** *103*, 3263-3296.
14. Proctor, R. S. J.; Colgan, A. C.; Phipps, R. J., Exploiting attractive non-covalent interactions for the enantioselective catalysis of reactions involving radical intermediates. *Nat. Chem.* **2020,** *12*, 990-1004.
15. Mondal, S.; Dumur, F.; Gigmes, D.; Sibi, M. P.; Bertrand, M. P.; Nechab, M., Enantioselective Radical Reactions Using Chiral Catalysts. *Chem. Rev.* **2022,** *122*, 5842-5976.
16. Emmanuel, M. A.; Greenberg, N. R.; Oblinsky, D. G.; Hyster, T. K., Accessing non-natural reactivity by irradiating nicotinamide-dependent enzymes with light. *Nature* **2016,** *540*, 414-417.

17. Huang, X.; Feng, J.; Cui, J.; Jiang, G.; Harrison, W.; Zang, X.; Zhou, J.; Wang, B.; Zhao, H., Photoinduced chemomimetic biocatalysis for enantioselective intermolecular radical conjugate addition. *Nat. Catal.* **2022,** *5*, 586-593.
18. Chen, B.; Li, R.; Feng, J.; Zhao, B.; Zhang, J.; Yu, J.; Xu, Y.; Xing, Z.; Zhao, Y.; Wang, B.; Huang, X., Modular Access to Chiral Amines via Imine Reductase-Based Photoenzymatic Catalysis. *J. Am. Chem. Soc.* **2024,** *146*, 14278-14286.
19. Sandoval, B. A.; Meichan, A. J.; Hyster, T. K., Enantioselective Hydrogen Atom Transfer: Discovery of Catalytic Promiscuity in Flavin-Dependent 'Ene'-Reductases. *J. Am. Chem. Soc.* **2017,** *139*, 11313-11316.
20. Black, M. J.; Biegasiewicz, K. F.; Meichan, A. J.; Oblinsky, D. G.; Kudisch, B.; Scholes, G. D.; Hyster, T. K., Asymmetric redox-neutral radical cyclization catalysed by flavin-dependent 'ene'-reductases. *Nat. Chem.* **2020,** *12*, 71-75.
21. Huang, X.; Wang, B.; Wang, Y.; Jiang, G.; Feng, J.; Zhao, H., Photoenzymatic enantioselective intermolecular radical hydroalkylation. *Nature* **2020,** *584*, 69-74.
22. Clayman, P. D.; Hyster, T. K., Photoenzymatic Generation of Unstabilized Alkyl Radicals: An Asymmetric Reductive Cyclization. *J. Am. Chem. Soc.* **2020,** *142*, 15673-15677.
23. Sandoval, B. A.; Clayman, P. D.; Oblinsky, D. G.; Oh, S.; Nakano, Y.; Bird, M.; Scholes, G. D.; Hyster, T. K., Photoenzymatic Reductions Enabled by Direct Excitation of Flavin-Dependent "Ene"-Reductases. *J. Am. Chem. Soc.* **2021,** *143*, 1735-1739.
24. Page, C. G.; Cooper, S. J.; DeHovitz, J. S.; Oblinsky, D. G.; Biegasiewicz, K. F.; Antropow, A. H.; Armbrust, K. W.; Ellis, J. M.; Hamann, L. G.; Horn, E. J.; Oberg, K. M.; Scholes, G. D.; Hyster, T. K., Quaternary Charge-Transfer Complex Enables Photoenzymatic Intermolecular Hydroalkylation of Olefins. *J. Am. Chem. Soc.* **2021,** *143*, 97-102.
25. Fu, H.; Lam, H.; Emmanuel, M. A.; Kim, J. H.; Sandoval, B. A.; Hyster, T. K., Ground-State Electron Transfer as an Initiation Mechanism for Biocatalytic C–C Bond Forming Reactions. *J. Am. Chem. Soc.* **2021,** *143*, 9622-9629.
26. Gao, X.; Turek-Herman, J. R.; Choi, Y. J.; Cohen, R. D.; Hyster, T. K., Photoenzymatic Synthesis of α-Tertiary Amines by Engineered Flavin-Dependent "Ene"-Reductases. *J. Am. Chem. Soc.* **2021,** *143* (47), 19643-19647.
27. Fu, H.; Cao, J.; Qiao, T.; Qi, Y.; Charnock, S. J.; Garfinkle, S.; Hyster, T. K., An asymmetric sp3–sp3 cross-electrophile coupling using 'ene'-reductases. *Nature* **2022,** *610*, 302-307.
28. Peng, Y.; Wang, Z.; Chen, Y.; Xu, W.; Hu, Y.; Chen, Z.; Xu, J.; Wu, Q., Photoinduced Promiscuity of Cyclohexanone Monooxygenase for the Enantioselective Synthesis of α-Fluoroketones. *Angew. Chem. Int. Ed.* **2022,** *61*, e202211199.
29. Zhang, Z.; Feng, J.; Yang, C.; Cui, H.; Harrison, W.; Zhong, D.; Wang, B.; Zhao, H., Photoenzymatic enantioselective intermolecular radical hydroamination. *Nat. Catal.* **2023,** *6*, 687-694.
30. Page, C. G.; Cao, J.; Oblinsky, D. G.; MacMillan, S. N.; Dahagam, S.; Lloyd, R. M.; Charnock, S. J.; Scholes, G. D.; Hyster, T. K., Regioselective Radical Alkylation of Arenes Using Evolved Photoenzymes. *J. Am. Chem. Soc.* **2023,** *145*, 11866-11874.
31. Chen, X.; Zheng, D.; Jiang, L.; Wang, Z.; Duan, X.; Cui, D.; Liu, S.; Zhang, Y.; Yu, X.; Ge, J.; Xu, J., Photoenzymatic Hydrosulfonylation for the Stereoselective Synthesis of Chiral Sulfones. *Angew. Chem. Int. Ed.* **2023,** *62*, e202218140.
32. Ouyang, Y.; Turek-Herman, J.; Qiao, T.; Hyster, T. K., Asymmetric Carbohydroxylation of Alkenes Using Photoenzymatic Catalysis. *J. Am. Chem. Soc.* **2023,** *145*, 17018-17022.
33. Duan, X.; Cui, D.; Wang, Z.; Zheng, D.; Jiang, L.; Huang, W.-Y.; Jia, Y.-X.; Xu, J., A Photoenzymatic Strategy for Radical-Mediated Stereoselective Hydroalkylation with Diazo Compounds. *Angew. Chem. Int. Ed.* **2023,** *62*, e202214135.
34. Fu, H.; Qiao, T.; Carceller, J. M.; MacMillan, S. N.; Hyster, T. K., Asymmetric C-Alkylation of Nitroalkanes via Enzymatic Photoredox Catalysis. *J. Am. Chem. Soc.* **2023,** *145*, 787-793.
35. Zhao, B.; Feng, J.; Yu, L.; Xing, Z.; Chen, B.; Liu, A.; Liu, F.; Shi, F.; Zhao, Y.; Tian, C.; Wang, B.; Huang, X., Direct visible-light-excited flavoproteins for redox-neutral asymmetric radical hydroarylation. *Nat. Catal.* **2023,** *6*, 996-1004.
36. Shi, Q.; Kang, X.-W.; Liu, Z.; Sakthivel, P.; Aman, H.; Chang, R.; Yan, X.; Pang, Y.; Dai, S.; Ding, B.; Ye, J., Single-Electron Oxidation-Initiated Enantioselective Hydrosulfonylation of Olefins Enabled by Photoenzymatic Catalysis. *J. Am. Chem. Soc.* **2024,** *146*, 2748-2756.
37. Li, M.; Harrison, W.; Zhang, Z.; Yuan, Y.; Zhao, H., Remote stereocontrol with azaarenes via enzymatic hydrogen atom transfer. *Nat. Chem.* **2023**, *16*, 277-284
38. Harrison, W.; Jiang, G.; Zhang, Z.; Li, M.; Chen, H.; Zhao, H., Photoenzymatic Asymmetric Hydroamination for Chiral Alkyl Amine Synthesis. *J. Am. Chem. Soc.* **2024,** *146*, 10716-10722.
39. Li, M.; Yuan, Y.; Harrison, W.; Zhang, Z.; Zhao, H., Asymmetric photoenzymatic incorporation of fluorinated motifs into olefins. *Science* **2024,** *385*, 416-421.
40. Liu, Y.; Bender, S. G.; Sorigue, D.; Diaz, D. J.; Ellington, A. D.; Mann, G.; Allmendinger, S.; Hyster, T. K., Asymmetric Synthesis of α-Chloroamides via Photoenzymatic Hydroalkylation of Olefins. *J. Am. Chem. Soc.* **2024,** *146*, 7191-7197.
41. Ju, S.; Li, D.; Mai, B. K.; Liu, X.; Vallota-Eastman, A.; Wu, J.; Valentine, D. L.; Liu, P.; Yang, Y., Stereodivergent photobiocatalytic radical cyclization through the repurposing and directed evolution of fatty acid photodecarboxylases. *Nat. Chem.* **2024**, *16*, 1339-1347, 42.
42. Raps, F. C.; Rivas-Souchet, A.; Jones, C. M.; Hyster, T. K., Emergence of a distinct mechanism of C–N bond formation in photoenzymes. *Nature* **2024,** 10.1038/s41586-024-08138-w.
43. Biegasiewicz, K. F.; Cooper, S. J.; Emmanuel, M. A.; Miller, D. C.; Hyster, T. K., Catalytic promiscuity enabled by photoredox catalysis in nicotinamide-dependent oxidoreductases. *Nat. Chem.* **2018,** *10*, 770-775.
44. Sandoval, B. A.; Kurtoic, S. I.; Chung, M. M.; Biegasiewicz, K. F.; Hyster, T. K., Photoenzymatic Catalysis Enables Radical‐Mediated Ketone Reduction in Ene‐Reductases. *Angew. Chem. Int. Ed.* **2019,** *58*, 8714-8718.
45. Nakano, Y.; Black, M. J.; Meichan, A. J.; Sandoval, B. A.; Chung, M. M.; Biegasiewicz, K. F.; Zhu, T.; Hyster, T. K., Photoenzymatic Hydrogenation of Heteroaromatic Olefins Using 'Ene'‐Reductases with Photoredox Catalysts. *Angew. Chem. Int. Ed.* **2020,** *59*, 10484-10488.
46. Ye, Y.; Cao, J.; Oblinsky, D. G.; Verma, D.; Prier, C. K.; Scholes, G. D.; Hyster, T. K., Using enzymes to tame nitrogen-centred radicals for enantioselective hydroamination. *Nat. Chem.* **2022**, *15*, 206–212.
47. Sun, S.-Z.; Nicholls, B. T.; Bain, D.; Qiao, T.; Page, C. G.; Musser, A. J.; Hyster, T. K., Enantioselective decarboxylative alkylation using synergistic photoenzymatic catalysis. *Nat. Catal.* **2023**, *7*, 35–42.

48. Cheng, L.; Li, D.; Mai, B. K.; Bo, Z.; Cheng, L.; Liu, P.; Yang, Y., Stereoselective amino acid synthesis by synergistic photoredox-pyridoxal radical biocatalysis. *Science* **2023,** *381*, 444-451.
49. Wang, T.-C.; Mai, B. K.; Zhang, Z.; Bo, Z.; Li, J.; Liu, P.; Yang, Y., Stereoselective amino acid synthesis by photobiocatalytic oxidative coupling. *Nature* **2024,** *629*, 98-104.
50. Wang, T.-C.; Zhang, Z.; Rao, G.; Li, J.; Shirah, J.; Britt, R. D.; Zhu, Q.; Yang, Y., Threonine Aldolase-Catalyzed Enantioselective α-Alkylation of Amino Acids through Unconventional Photoinduced Radical Initiation. *J. Am. Chem. Soc.* **2024,** *146*, 22476–22484.
51. Ouyang, Y.; Page, C. G.; Bilodeau, C.; Hyster, T. K., Synergistic Photoenzymatic Catalysis Enables Synthesis of a-Tertiary Amino Acids Using Threonine Aldolases. *J. Am. Chem. Soc.* **2024,** *146*, 13754-13759.
52. Yu, J.; Zhang, Q.; Zhao, B.; Wang, T.; Zheng, Y.; Wang, B.; Zhang, Y.; Huang, X., Repurposing Visible-Light-Excited Ene-Reductases for Diastereo- and Enantioselective Lactones Synthesis. *Angew. Chem. Int. Ed.* **2024,** e202402673.
53. Xu, Y.; Chen, H.; Yu, L.; Peng, X.; Zhang, J.; Xing, Z.; Bao, Y.; Liu, A.; Zhao, Y.; Tian, C.; Liang, Y.; Huang, X., A light-driven enzymatic enantioselective radical acylation. *Nature* **2024,** *625*, 74-78.
54. Liu, X.; Xu, S.; Chen, H.; Yang, Y., Unnatural Thiamine Radical Enzymes for Photobiocatalytic Asymmetric Alkylation of Benzaldehydes and α-Ketoacids. *ACS Catal.* **2024**, 9144-9150.
55. Ding, Y.; Ting, J. P.; Liu, J.; Al-Azzam, S.; Pandya, P.; Afshar, S., Impact of non-proteinogenic amino acids in the discovery and development of peptide therapeutics. *Amino Acids* **2020,** *52*, 1207-1226.
56. Blaskovich, M. A. T., Unusual Amino Acids in Medicinal Chemistry. *J. Med. Chem.* **2016,** *59*, 10807-10836.
57. Hickey, J. L.; Sindhikara, D.; Zultanski, S. L.; Schultz, D. M., Beyond 20 in the 21st Century: Prospects and Challenges of Non-canonical Amino Acids in Peptide Drug Discovery. *ACS Med. Chem. Lett.* **2023,** *14*, 557-565.
58. Hedges, J. B.; Ryan, K. S., Biosynthetic Pathways to Nonproteinogenic alpha-Amino Acids. *Chem. Rev.* **2020,** *120*, 3161-3209.
59. Lang, K.; Chin, J. W., Cellular Incorporation of Unnatural Amino Acids and Bioorthogonal Labeling of Proteins. *Chem. Rev.* **2014,** *114*, 4764-4806.
60. Dumas, A.; Lercher, L.; Spicer, C. D.; Davis, B. G., Designing logical codon reassignment–Expanding the chemistry in biology. *Chem. Sci.* **2015,** *6*, 50-69.
61. Birch-Price, Z.; Hardy, F. J.; Lister, T. M.; Kohn, A. R.; Green, A. P., Noncanonical Amino Acids in Biocatalysis. *Chem. Rev.* **2024,** *124*, 8740-8786.
62. De Faveri, C.; Mattheisen, J. M.; Sakmar, T. P.; Coin, I., Noncanonical Amino Acid Tools and Their Application to Membrane Protein Studies. *Chem. Rev.* **2024**, 10.1021/acs.chemrev.4c00181Chem.
63. Dunkelmann, D. L.; Chin, J. W., Engineering Pyrrolysine Systems for Genetic Code Expansion and Reprogramming. *Chem. Rev.* **2024,** *124*, 11008-11062.
64. Feng, R.-r.; Wang, M.; Zhang, W.; Gai, F., Unnatural Amino Acids for Biological Spectroscopy and Microscopy. *Chem. Rev.* **2024,** *124*, 6501-6542.
65. Eliot, A. C.; Kirsch, J. F., Pyridoxal Phosphate Enzymes: Mechanistic, Structural, and Evolutionary Considerations. *Annu. Rev. Biochem.* **2004,** *73*, 383-415.
66. Almhjell, P. J.; Boville, C. E.; Arnold, F. H., Engineering enzymes for noncanonical amino acid synthesis. *Chem. Soc. Rev.* **2018,** *47*, 8980-8997.
67. Steffen-Munsberg, F.; Vickers, C.; Kohls, H.; Land, H.; Mallin, H.; Nobili, A.; Skalden, L.; van den Bergh, T.; Joosten, H.-J.; Berglund, P.; Höhne, M.; Bornscheuer, U. T., Bioinformatic analysis of a PLP-dependent enzyme superfamily suitable for biocatalytic applications. *Biotechnol. Adv.* **2015,** *33*, 566-604.
68. Nájera, C.; Sansano, J. M., Catalytic Asymmetric Synthesis of α-Amino Acids. *Chem. Rev.* **2007,** *107*, 4584-4671.
69. Phillips, R. S., Synthetic applications of tryptophan synthase. *Tetrahedron: Asymmetry* **2004,** *15*, 2787-2792.
70. Watkins-Dulaney, E.; Straathof, S.; Arnold, F., Tryptophan Synthase: Biocatalyst Extraordinaire. *ChemBioChem* **2021,** *22*, 5-16.
71. Goss, R. J. M.; Newill, P. L. A., A convenient enzymatic synthesis of l-halotryptophans. *Chem. Commun.* **2006**, 4924-4925.
72. Buller, A. R.; Brinkmann-Chen, S.; Romney, D. K.; Herger, M.; Murciano-Calles, J.; Arnold, F. H., Directed evolution of the tryptophan synthase β-subunit for stand-alone function recapitulates allosteric activation. *Proc. Natl. Acad. Sci. U.S.A.* **2015,** *112*, 14599-14604.
73. Herger, M.; Van Roye, P.; Romney, D. K.; Brinkmann-Chen, S.; Buller, A. R.; Arnold, F. H., Synthesis of β-Branched Tryptophan Analogues Using an Engineered Subunit of Tryptophan Synthase. *J. Am. Chem. Soc.* **2016,** *138*, 8388-8391.
74. Holmes, J. B.; Liu, V.; Caulkins, B. G.; Hilario, E.; Ghosh, R. K.; Drago, V. N.; Young, R. P.; Romero, J. A.; Gill, A. D.; Bogie, P. M.; Paulino, J.; Wang, X.; Riviere, G.; Bosken, Y. K.; Struppe, J.; Hassan, A.; Guidoulianov, J.; Perrone, B.; Mentink-Vigier, F.; Chang, C.-e. A.; Long, J. R.; Hooley, R. J.; Mueser, T. C.; Dunn, M. F.; Mueller, L. J., Imaging active site chemistry and protonation states: NMR crystallography of the tryptophan synthase α-aminoacrylate intermediate. *Proc. Natl. Acad. Sci. U.S.A.* **2022,** *119*, e2109235119.
75. Huang, Y.-m. M.; You, W.; Caulkins, B. G.; Dunn, M. F.; Mueller, L. J.; Chang, C.-e. A., Protonation states and catalysis: Molecular dynamics studies of intermediates in tryptophan synthase. *Protein Sci.* **2016,** *25*, 166-183.
76. Fesko, K., Threonine aldolases: perspectives in engineering and screening the enzymes with enhanced substrate and stereo specificities. *Appl. Microbiol. Biotechnol.* **2016,** *100*, 2579-2590.
77. Dückers, N.; Baer, K.; Simon, S.; Gröger, H.; Hummel, W., Threonine aldolases—screening, properties and applications in the synthesis of non-proteinogenic β-hydroxy-α-amino acids. *Appl. Microbiol. Biotechnol.* **2010,** *88*, 409-424.
78. Du, S.; Wey, M.; Armstrong, D. W., D-Amino acids in biological systems. *Chirality* **2023**, *35*, 508-534..
79. Pollegioni, L.; Rosini, E.; Molla, G. Advances in Enzymatic Synthesis of D-Amino Acids. *J. Mol. Sci.* **2020**, *21*, 3206
80. Tellis, J. C.; Primer, D. N.; Molander, G. A., Single-electron transmetalation in organoboron cross-coupling by photoredox/nickel dual catalysis. *Science* **2014,** *34*, 433-436.
81. Chovancova, E.; Pavelka, A.; Benes, P.; Strnad, O.; Brezovsky, J.; Kozlikova, B.; Gora, A.; Sustr, V.; Klvana, M.; Medek, P.; Biedermannova, L.; Sochor, J.; Damborsky, J., CAVER 3.0: A

Tool for the Analysis of Transport Pathways in Dynamic Protein Structures. *PLoS Comput. Biol.* **2012,** *8*, e1002708.
82. Kille, S.; Acevedo-Rocha, C. G.; Parra, L. P.; Zhang, Z.-G.; Opperman, D. J.; Reetz, M. T.; Acevedo, J. P., Reducing Codon Redundancy and Screening Effort of Combinatorial Protein Libraries Created by Saturation Mutagenesis. *ACS Synth. Biol.* **2013,** *2*, 83-92.
83. Gillis, E. P.; Burke, M. D., A Simple and Modular Strategy for Small Molecule Synthesis: Iterative Suzuki–Miyaura Coupling of B-Protected Haloboronic Acid Building Blocks. *J. Am. Chem. Soc.* **2007,** *129*, 6716-6717.
84. Gonzalez, J. A.; Ogba, O. M.; Morehouse, G. F.; Rosson, N.; Houk, K. N.; Leach, A. G.; Cheong, P. H. Y.; Burke, M. D.; Lloyd-Jones, G. C., MIDA boronates are hydrolysed fast and slow by two different mechanisms. *Nat. Chem.* **2016,** *8*, 1067-1075.
85. Lennox, A. J. J.; Lloyd-Jones, G. C., Organotrifluoroborate Hydrolysis: Boronic Acid Release Mechanism and an Acid–Base Paradox in Cross-Coupling. *J. Am. Chem. Soc.* **2012,** *134*, 7431-7441.
86. Gary, S.; Landry, M.; Bloom, S., Spectral and Electrochemical Properties of Common Photocatalysts in Water: A Compendium for Aqueous Photoredox Catalysis. *Synlett* **2023,** *34*, 1911-1914.
87. Chilamari, M.; Immel, J. R.; Bloom, S., General Access to C-Centered Radicals: Combining a Bioinspired Photocatalyst with Boronic Acids in Aqueous Media. *ACS Catal.* **2020,** *10*, 12727-12737.
88. Lima, F.; Kabeshov, M. A.; Tran, D. N.; Battilocchio, C.; Sedelmeier, J.; Sedelmeier, G.; Schenkel, B.; Ley, S. V., Visible Light Activation of Boronic Esters Enables Efficient Photoredox C(sp^2)-C(sp^3) Cross-Couplings in Flow. *Angew. Chem. Int. Ed.* **2016,** *128*, 14291-14295.
89. Lima, F.; Sharma, U. K.; Grunenberg, L.; Saha, D.; Johannsen, S.; Sedelmeier, J.; Van Der Eycken, E. V.; Ley, S. V., A Lewis Base Catalysis Approach for the Photoredox Activation of Boronic Acids and Esters. *Angew. Chem. Int. Ed.* **2017,** *56*, 15136-15140.
90. Shaw, J. P.; Petsko, G. A.; Ringe, D., Determination of the Structure of Alanine Racemase from Bacillus stearothermophilus at 1.9-Å Resolution. *Biochemistry* **1997,** *36*, 1329-1342.
91. Sun, S.; Toney, M. D., Evidence for a Two-Base Mechanism Involving Tyrosine-265 from Arginine-219 Mutants of Alanine Racemase. *Biochemistry* **1999,** *38*, 4058-4065.
92. Spies, M. A.; Toney, M. D., Multiple Hydrogen Kinetic Isotope Effects for Enzymes Catalyzing Exchange with Solvent: Application to Alanine Racemase. *Biochemistry* **2003,** *42*, 5099-5107.
93. Chan-Huot, M.; Dos, A.; Zander, R.; Sharif, S.; Tolstoy, P. M.; Compton, S.; Fogle, E.; Toney, M. D.; Shenderovich, I.; Denisov, G. S.; Limbach, H.-H., NMR Studies of Protonation and Hydrogen Bond States of Internal Aldimines of Pyridoxal 5'-Phosphate Acid − Base in Alanine Racemase, Aspartate Aminotransferase, and Poly-L-lysine. *J. Am. Chem. Soc.* **2013,** *135*, 18160-18175.

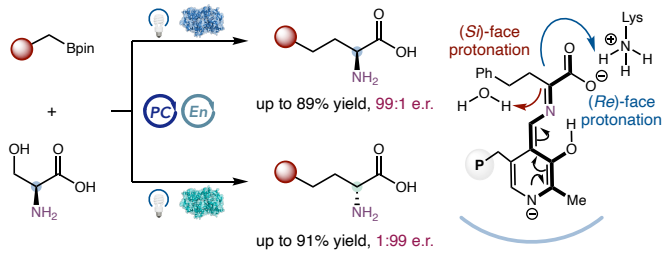

■ **PLP radical biocatalysis** ■ **Enantiodivergent amino acid synthesis** ■ **Mechanism**